

Stiffness analysis for a 3-PUU parallel kinematic machine

S.VEERENDRA PRASAD, DR.V.V.SUBBA RAO, DR.B.V.R.RAVI KUMAR,

Research Scholar, JNTUK and Assistant professor, Principal, Professor,

Department of Mechanical Engineering,

Samskruti College of Engineering and Technology, Ghatkesar.

Abstract

This paper describes the stiffness characteristics of a 3-PUU translational parallel kinematic machine (PKM). An alternative method of generating the stiffness matrix is used when considering actuators and limitations, as well as the compliances of both actuators and legs. Extreme stiffness values and their design consequences are used to evaluate rigidity manipulator performance.

Using the stiffness of a 3-PUU PKM in the design of its architecture is a good idea. Using an eigenscrew decomposition of the PKM's stiffness matrix, it is possible to identify the PKM's stiffness centre and the PKM's compliant axis, which provides a physical interpretation of PKM stiffness.

Stiffness; workspace; parallel manipulator mechanics and design

Introduction

Because of all the various applications, parallel manipulators have become more popular in recent years [1]. Parallel manipulators with fewer than six degrees of freedom (DOF) have been extensively employed in many applications due to the inherent advantages of parallel mechanisms while also giving additional benefits in terms of manufacturing and operating expenses. Sturdiness is critical for parallel mechanisms since they increase cutting speeds and enhance the accuracy of the end-effector. Because the stiffness of a parallel kinematic machine has to be measured and assessed as early in the design process as feasible (PKM). Prior to the 3-PUU mechanism, the concept of translational parallelism was raised and researched [5–6]. There has been minimal investigation on the entire stiffness of the system, despite the fact that actuators and legs have their own compliance. PKM in motion is examined to see how the structure's dynamics are affected by a 3-PUU PKM stiffness model developed for this study.

Section 1.1 discusses stiffness modelling.

This connection between force and deflection is linear when elastic devices support a rigid body [7], as defined by a 6x6 positive semidefinite matrix that is symmetrical. End-vector effector of compliant deformations is connected to a static external wrench via a 6x6 stiffness matrix to identify parallel manipulators. Six-leg parallel 6-DOF manipulators with pliability of each compliant portion may be utilised to construct a basic stiffness model. It takes a long time to create stiffness maps for manipulators with just two degrees of freedom. The stiffness of a tripod-based PKM may be mimicked via virtual labour [10]. In [11], a parallel manipulator model for CaPaMan was created by using the kinematic and static features of all three legs.

Present methodologies are inadequate to explain the stiffness of manipulators with fewer degrees of freedom of motion. Prior to this work, methods to construct a parallel manipulator's stiffness matrix using an overall Jacobian were suggested [12]. The 6 x 6 matrix of a translational PKM may summarise the stiffness and restrictions of the actuators of a less-DOF parallel manipulator, according to this work.

Stiffness assessment,

The design of the workspace and the direction in which wrenches are applied determine the stiffness of a PKM for a particular set of manipulator parameters. When assessing whether or not the design complies with stiffness criteria or even performs an ideal design, a model of the object's stiffness must be constructed and predicted. To have a deeper understanding of a PKM's stiffness behaviour, it must be tested in many configurations. For measuring stiffness, many performance indicators have been established and used in the literatures. The stiffness matrix terms [8,10] may be used to get an idea of how stiff something is. It is also possible to evaluate stiffness by looking at the stiffness matrix's eigenvalue for the eigenvector in question [8,13]. According to the findings of researchers, a rigidity limit exists for stiffness matrices with low and high Eigenvalues. [14] The largest to smallest eigenvalue ratio of the stiffness matrix may be used to forecast stiffness values. There are several ways to evaluate the stiffness matrix, including its determinant, which is the product of its eigenvalues [5,11]. A three-dof spherical parallel manipulator's stiffness may be evaluated using a stiffness matrix divided by the workspace volume [15].

It is unable to effectively describe the stiffness attribute in any direction because of off-diagonal components in the general form of stiffness matrix. Determinant or trace values are very high even though the manipulator's low stiffness prevents it from being used in applications since or trace cannot differentiate the difference.

However, even if the condition number indicates that the stiffness matrix has been improperly prepared for consistent manipulation, a machine tool must have a minimum stiffness level across its workspace. As a result, in this article, performance is measured using the lowest and maximum stiffness values, as well as their variations.

The stiffness model of a PKM is essential for understanding the PKM's spatial compliance. It is possible to provide a physical explanation for spatial elastic behaviour if the stiffness matrix is divided into its component eigenscrews. If the stiffness centre and compliant axis are present, this physical interpretation is plausible [18]. RCC (remote centre of compliance) idea may be extended to include off-diagonal blocks diagonalized at the centre of stiffness in stiffness matrix definition. This decoupling of rotation and translation is still conceivable if the normal form for generic stiffness matrices is not diagonal. It is used in robotics as a torsional and linear spring in the same device. When applied to the axis of a compliant system, both linear and rotational deformation are parallel. Even in a strict system, this is the case.

Section 2 introduces the 3-PUU PKM, whereas Section 3 explains a new method for calculating the stiffness matrix. Section 4 employs shock indices to forecast the influence of design

components on the structural integrity of a product. Section 5 concludes the discussion with a few last observations.

Kinematic description

Figure 1 depicts the CAD model of a 3-PUU PKM, whereas Figure 2 shows the schematic design. A movable platform, a stationary base, and three arms with the same kinematic framework make up the manipulator. Lead screw linear actuators are used to drive (U) joints sequentially. Because each U joint is made up of two revolute (R) joints that meet at an angle, each limb may move like a Chain of motion PRRRR. Only translational movements can be achieved using a 3-PUU mechanism.

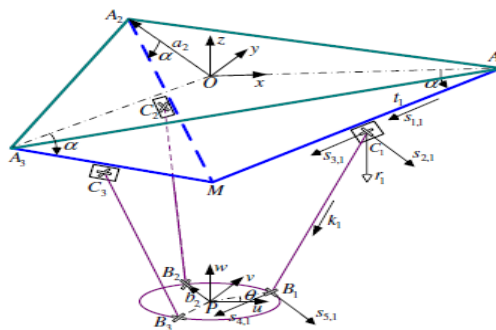


Fig. 2. Schematic representation of a 3-PUU PKM.

For each chain, the initial and last revolute joints are parallel, and the two intermediate joint axes are also parallel. Figure 2 shows the fixed Cartesian reference frame (Ox,y,z) we'll be using for this inquiry. The permanent base of the platform and the movable frame of the mobile platform. Triangle DB1A2B3 and triangle DB1B2B3 intersecting. The x and u axes should be aligned to make things easy. OA1 is used to designate the x-axis. Oai and OAi are the vectors' angles to each other. PBi "1; 2; 3" is a novel way of putting it. Angle h, therefore, is the angle formed by a moving platform and a stationary base. On one of its three tracks, AiM crosses across. The x-y plane has three points where circles of the same radius intersect: A1, A2, and A3, as well as M, where a third circle of the same radius crosses. Circles B1, B2, and B3 are the intersection locations of the three legs CiBi with lengths l in the U-V plane. Its circumference is b. Angle an is defined as the angle of motion of the actuators from the base to the rails AiM. Perspective. To guarantee that the manipulator has a symmetric workspace, DA1A2A3 and DB1B2B3 must be used. Equilateral triangles are being distributed. Leg CiBi represents the actuator's linear displacement and its rotation. An indicator of the unit vector should be shown on the AiM rail. Make sure ai gets a quarter of OAi, too. One-eighth PBI is an alternative. For every time, there is a four-fold multiplier. Vector-loop analysis may be used to address both forward and backward motion issues. Closed-form solutions may exist. Solutions to inverted kinematics may be summed up as follows: As a result of this data, the 3-PUU PKM's workspace is now revealed.

$$d_i = h^T e_i - \sqrt{(h^T e_i)^2 - e_i^T e_i + l^2} \quad (1)$$

where $e_i = p + b_i - a_i$, for $i = 1, 2, \text{ and } 3$.

Stiffness matrix generation

Jacobian matrix derivation

The Jacobian matrix of a parallel manipulator may be derived using reciprocal screw theory [12]. The mobile platform's twist may be described as $T = tT + xTT$ in Plucker axis coordinates, with t and x designating the vectors for linear and angular velocities, respectively.

$$T = \dot{d}_1 \hat{T}_{1j} + \dot{\theta}_2 \hat{T}_{2j} + \dot{\theta}_3 \hat{T}_{3j} + \dot{\theta}_4 \hat{T}_{4j} + \dot{\theta}_5 \hat{T}_{5j} \quad (2)$$

A unit screw (in Plucker coordinates) is connected with each of the joints of the leg in which the intensity is equal to or greater than \hat{t}_{ij} , where i is 1, 2, or 3.

$$\hat{T}_{1j} = \begin{bmatrix} s_{1j} \\ 0 \\ 0 \end{bmatrix}, \hat{T}_{2j} = \begin{bmatrix} c_j \times s_{2j} \\ s_{2j} \\ 0 \end{bmatrix}, \hat{T}_{3j} = \begin{bmatrix} c_j \times s_{3j} \\ s_{3j} \\ 0 \end{bmatrix}, \hat{T}_{4j} = \begin{bmatrix} b_j \times s_{4j} \\ s_{4j} \\ 0 \end{bmatrix}, \hat{T}_{5j} = \begin{bmatrix} b_j \times s_{5j} \\ s_{5j} \\ 0 \end{bmatrix}$$

The following equations are used to determine \hat{t}_{ij} . For the 3-PUU mechanism's joint axis, the translational PKM has to fulfil criteria $s_{3j} > 0$. First, a ray coordinate of one screw \hat{t}_{ij} , which is reciprocal to all other screws \hat{T}_{kj} of the i th joint. Secondly, a ray coordinate A_1 -system is a screw with an infinite pitch that is oriented perpendicular to the limb. The articulation of a U-joint is divided into two axes:

$$\hat{t}_{ij} = \begin{bmatrix} 0 \\ r_j \end{bmatrix}, \quad (3)$$

Eq. (2) may be constructed into a matrix form by taking the product of both sides of the equation with \hat{t}_{ij} .

$$J_c T = 0, \quad (4)$$

where

$$J_c = \begin{bmatrix} 0 & r_1^T \\ 0 & r_2^T \\ 0 & r_3^T \end{bmatrix}_{3 \times 6} \quad (5)$$

is referred to as the Jacobian principle of constraint. The mobile platform's 3-DOF mobility is restricted by the combination of the limitations in each row of J_c . The unique solution to Eq. (4) if r_i is: $x \neq 0$. This system contains the, Screw \hat{t}_{ij} had already figured it out. All the passive joint screws of the extra basis screws \hat{T}_{kj} are reciprocal zero pitch screw may be distinguished along the path of the two U joints, i.e.

$$\hat{t}_{ij} = \begin{bmatrix} k_j \\ b_j \times k_j \end{bmatrix}. \quad (6)$$

Similarly, taking the product of both sides of Eq. (2) with \hat{t}_{ij} , leads to a matrix-form result:

$$J_d \dot{q} = \dot{q}_i, \quad (7)$$

where $\dot{q} = [\dot{d}_1 \ \dot{\theta}_2 \ \dot{\theta}_3]^T$ denotes the actuated joint rate and

$$J_d = \begin{bmatrix} \frac{k_j^T}{k_j^T s_{1j}} & \frac{(b_j \times k_j)^T}{k_j^T s_{1j}} \\ \frac{k_j^T}{k_j^T s_{2j}} & \frac{(b_j \times k_j)^T}{k_j^T s_{2j}} \\ \frac{k_j^T}{k_j^T s_{3j}} & \frac{(b_j \times k_j)^T}{k_j^T s_{3j}} \end{bmatrix}_{3 \times 6} \quad (8)$$

it's known as the Jacobian of motions. Ja's units demonstrate following talks. As a result, in order to construct a stiffness matrix, the Jacobian matrix units must be homogenised. Invariant to the length unit selected, the performance index The dimensionally homogenous Jc is dimensionless. It is possible to attain the Jacobian of actuations

$$J_{ab} = J_a W \quad (9)$$

with $W = \text{diag}[1, 1, 1, \frac{1}{b}, \frac{1}{b}, \frac{1}{b}]$, where the mobile platform radius b is chosen as the characteristic length to homogenize the dimension of the Jacobian matrix.

Combining Eqs. (4) and (7) allows the generation of

$$\dot{q}_0 = J T, \quad (10)$$

where $\dot{q}_0 = [\dot{d}_1 \ \dot{d}_2 \ \dot{d}_3 \ 0 \ 0 \ 0]^T$ is the extended joint rate, and

$$J = \begin{bmatrix} J_{ab} \\ J_c \end{bmatrix}_{6 \times 6} \quad (11)$$

is called the overall Jacobian of a 3-PUU PKM, which is homogeneous in terms of units.

Stiffness modelling is discussed in section

Three constraint couples are exerted on the movable platform by the wrench system that is the reciprocal screw system with infinite pitch and by the reciprocal screw system with zero pitch. Three forces are applied to the movable platform via the screw system of actuation. the limbs. In other words, each leg is subjected to one and a half times its own weight in a certain direction. Considering the premise Infinite rigidity of the U joints and mobile platform and the compliance of actuators and legs are the only constraints may be deduced in this manner.

Control of actuators affects compliance

To move a lead screw, the torque must be transmitted between the i th nut and the linear displacement may be estimated as a function of time

$$f_i = \frac{2\tau_i}{\mu_c d_s} \quad \text{and} \quad \Delta l_i = \frac{p \tau_i}{K_{s_i}} \quad (12)$$

Assume that μ_c is the friction coefficient of the i th actuator, s_i is its torsional stiffness, and d_s is its pitch diameter. According to Eq. (12), one can calculate the linear driving device's compliance:

$$C_i = \frac{\Delta l_i}{f_i} = \frac{\mu_c d_s p}{2K_{s_i}} \quad (13)$$

As a result, the projection of compliance in the corresponding leg's direction may be deduced as a function of the i th actuator.

$$C_{ij}^k = k_i^T s_{ij} C_i \quad (14)$$

Legs-based compliance

Transverse compliance is equal to the i th leg's $C_{kl};i$, whereas longitudinal compliance is the same. There is an elastic deformation of the i th leg because of a constraint force F_{ki} and a

constraint couple M_i perpendicular to the limb's universal joint. This means that the elastic deformations may be represented as follows:

$$\Delta l_i = C_{l_i}^k F_i^k = \frac{l}{AE} F_i^k, \quad (15)$$

$$\Delta \theta_i = C_{\theta_i}^k M_i^k = \frac{l}{GI_p} k_i^T r_i M_i^k, \quad (16)$$

There are two legs, each with a length of l and a cross-sectional area of A , and each leg has a modulus of elasticity E and G , respectively. Eqs. (15) and (16) may then be used to generate C_{k_i} and C_{k_h} .

The stiffness model

Constraints' and actuators' stiffnesses may be calculated using the inverse connection between stiffness and compliance

$$K_{a,i} = C_{a,i}^{-1} = (C_{a,i}^k + C_{l,i}^k)^{-1}, \quad (17a)$$

$$K_{c,i} = C_{c,i}^{-1} = (C_{\theta,i}^k)^{-1} \quad (17b)$$

for $i = 1, 2, \text{ and } 3$.

Consider that three linear springs are used to link the movable platform to the stationary base, and three rotating springs are used as well, as shown in Fig.

Stiffness matrix determination

Suppose an external wrench w is applied to the movable platform in the form of the Plücker ray coordinate, where force is denoted by the notation F , torque is denoted by the notation M , and so on. The response forces/torques of the actuators and restraints, respectively, may be represented by the s_a and s_c symbols. Reaction forces/torques exerted by actuators and restraints, i.e., the external wrench is balanced in the absence of gravity

$$w = J_a^T \tau_a + J_c^T \tau_c, \quad (18)$$

where the reaction forces/moments can be expressed as

$$\tau_a = K_a \Delta q_a, \quad (19a)$$

$$\tau_c = K_c \Delta q_c, \quad (19b)$$

the matrices are $v_a = \text{diag}\{1, 2, 3\}$; $K_a = 2-3$ and v_c , respectively, which represent the displacements of actuations and restrictions, respectively, in the form of D_{q_a} and D_{q_c} . It is also possible to calculate the displacements of translation and rotation of the movable platform with respect to the three reference axes by using the formula: $dx, dy, dz, \theta_x, \theta_y, \theta_z$. Then, by ignoring the gravitational impact, the formation of virtual labour is possible.

$$w^T \Delta X = \tau_a^T \Delta q_a + \tau_c^T \Delta q_c, \quad (20)$$

where $\Delta X = [\Delta x^T \Delta \theta^T]^T$ denotes the mobile platform's twist deformation in the axis coordinate.

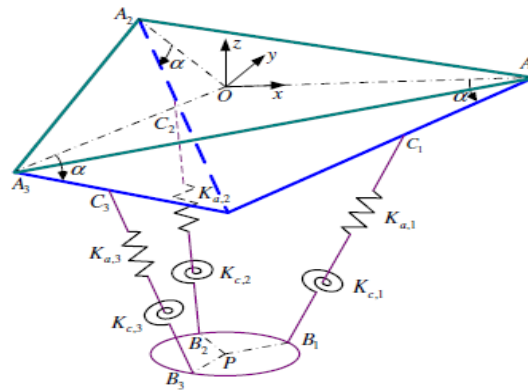


Fig. 3. Stiffness model of a 3-PUU PKM.

A careful analysis of Eqs. (18)–(20) at the same time, leads to the expression of

$$w = K \Delta X, \quad (21)$$

in where K is defined as the 6-by-6 overall stiffness matrix of a 3-PUU PKM, encompassing the influence of actuations and restrictions, with the 6-by-6 diagonal matrix v $\text{diag}(v_1, v_2, v_3, v_4, v_5, v_6)$. Where

Evaluation of the 3-PUU PKM's stiffness

As can be seen in Table 1, the 3-PUU PKM's design parameters aim to strike a balance between the overall workspace's global dexterity index and the space utility ratio index, which measures the workspace's volume in relation to the robot's physical size [6]. In addition, the U joints' cone angle restrictions are 20° , and the P joints' motion range limits are ± 0.1 m. The manipulator's accessible workspace is constructed as illustrated in Fig. 4 using a numerical search approach described in [19]. Moreover, Table 2 details the design's physical properties (3-PUU PKM). $(0, 0, 0)$ is the home position of the mobile platform in the case of mid-stroke linear actuators, in which the stiffness matrix is derived as follows:

Table 1
Architectural parameters of a 3-PUU PKM

Parameter	Value
a	0.3 m
b	0.1 m
l	0.3 m
α	45.0°
θ	0.0°

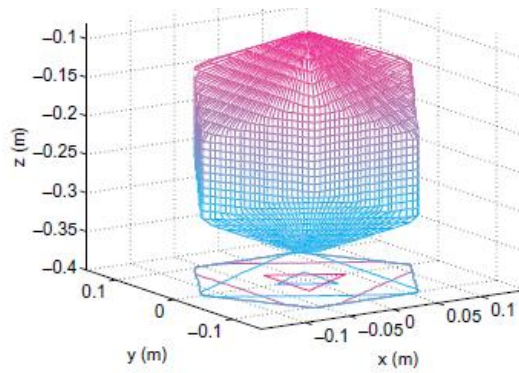


Fig. 4. Reachable workspace of a 3-PUU PKM.

Table 2
Physical parameters of a 3-PUU PKM

Parameter	Value	Parameter	Value
$K_{s,i}$	$1.45 \times 10^6 \text{ N/m/rad}$	E	$2.03 \times 10^{11} \text{ N/m}^2$
μ_c	0.25	G	$7.85 \times 10^{10} \text{ N/m}^2$
d_i	20 mm	A	$2.01 \times 10^{-4} \text{ m}^2$
p	3 mm	I_p	$3.22 \times 10^{-8} \text{ m}^4$

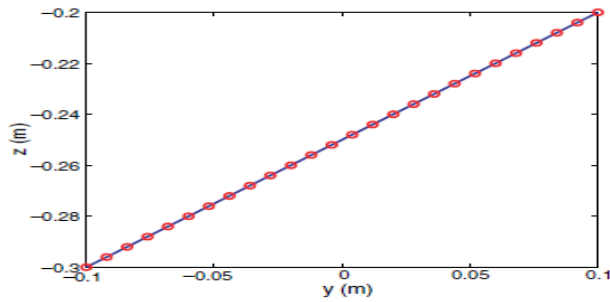


Fig. 5. Trajectory of the mobile platform in a plane of $x = 0 \text{ m}$.

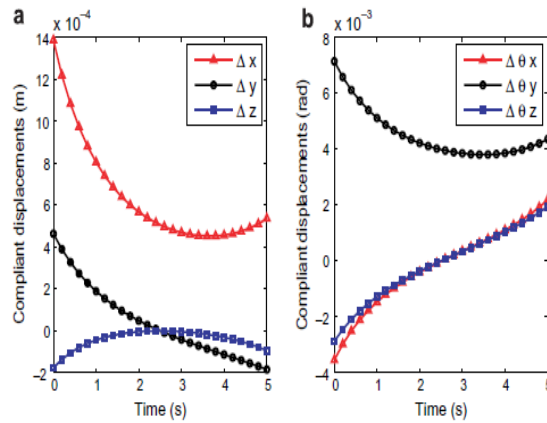


Fig. 6. The compliant displacements of (a) translations and (b) rotations of the mobile platform.

$$K^0 = \begin{bmatrix} 9.0891 & 0 & 0 & 0 & -1.0162 & 0 \\ 0 & 9.0891 & 0 & 1.0162 & 0 & 0 \\ 0 & 0 & 22.7228 & 0 & 0 & 0 \\ 0 & 1.0162 & 0 & 0.1137 & 0 & 0 \\ -1.0162 & 0 & 0 & 0 & 0.1137 & 0 \\ 0 & 0 & 0 & 0 & 0 & 0.0001 \end{bmatrix} \times 10^7,$$

Words N/m are used in this context to describe the phrases K0 11g; K113g; and N/rad to describe the phrases N/mg; K015g; and N/mg. PKM's movable platform may be utilised to calculate the DX's compliant displacement in light of Equation (21). As seen in FIG. 6, the platform moves at a constant speed while being exposed to a static external force of 20 N. It was found that the linear compliant displacement along the x-axis was 1.4 mm, as predicted. In addition to this, the y-axis rotation is the most rotary-compliant displacement of them all.

Stiffness assessment

PKM manipulation requires a stiffer workspace than a defined threshold. An overall perspective of the workspace's stiffness levels may be gained via deriving the lowest and greatest stiffness eigenvalues using classical eigenvalue decomposition. The total stiffness of the PKM workspace was measured numerically. Volume V division in cartesian coordinates as well as an evaluation of individual pieces to decide whether or not they belong in the workspace are critical components of this method. The size of the samples required depends on the level of precision. Mechanical joint motion restrictions and inverse kinematic solutions are used for verification. Decomposition of a stiffness matrix yields the parts that lie inside a certain workspace's boundaries. For each sample, the lowest and greatest stiffness values are compared to determine the workspace's minimum and maximum stiffness values. It has been employed because it is simple to implement in a computer programme. [20] A Gough-type parallel manipulator may benefit from a computer round-off analysis technique. It may also be used to build and compare two 3-DOF PKMs [3].

Figure 7 illustrates the stiffness levels in the $z = 0.242$ m (home position height) planes. There are three P joints with 120 degree x-y rotations in the viewing workspace, as shown. In addition, a manipulator's minimum stiffness and maximum stiffness increase as it approaches the workspace border. When employed outside of the attainable workspace, the PKM has poor stiffness qualities. It makes sense to keep it there. This subworkspace's definition is determined by the PKM tasks and performance metrics. Workspace is divided into a cubic shape with a 0.01 m edge length, with the platform's home location specified as the centre. " Stiffness is examined by changing the kinematic parameters. As little as 0.002 millimetres in diameter, the stiffness of this workspace may be determined. In Figs. 8a-d, the 3-PUU PKM's stiffness varies somewhat, which is consistent with the 3-PUU PKM's design parameters.

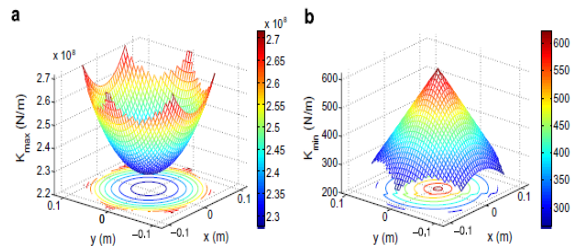
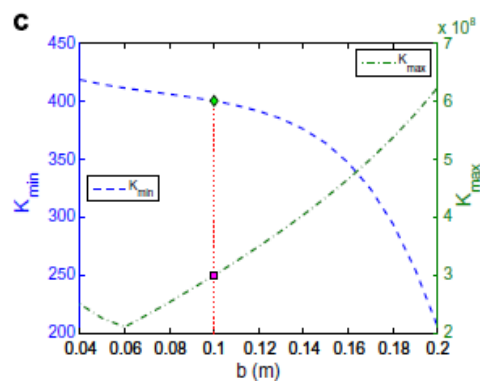
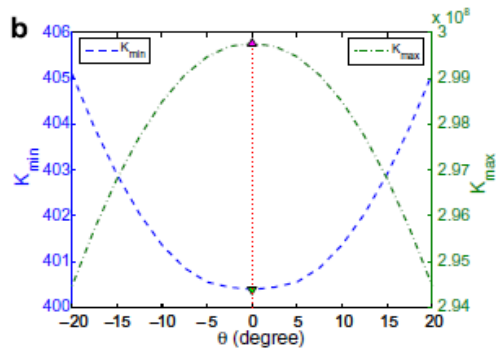
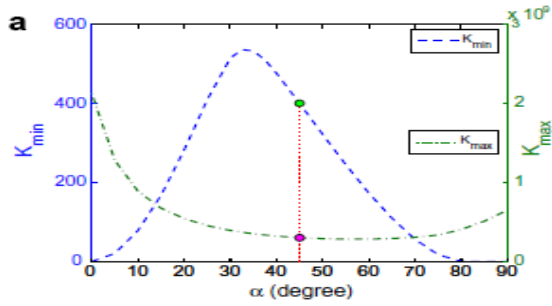


Fig. 7. The distribution for (a) minimum and (b) maximum stiffness in a plane of $z = -0.224$ m.



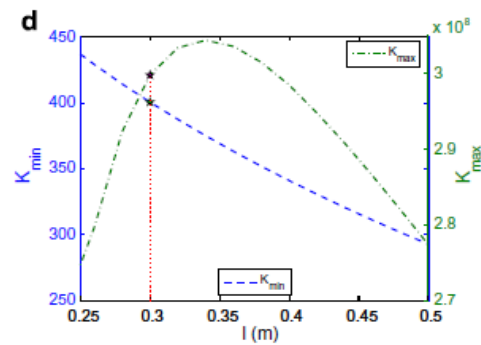


Fig. 8. Global stiffness index versus design parameters of (a) actuators layout angle, (b) twist angle, (c) mobile platform size, and (d) the leg length.

The manipulator's rigidity must be taken into account. Between 0 and 90 degrees, the minimum stiffness seems to peak between 30 and 35 degrees, while the maximum stiffness appears to reach its lowest value around 60 degrees. Minimum and maximum stiffness values are lowest for twist angles of h 14 0 when the moveable platform size grows from 0.25 metres to 0.50 metres, while maximum stiffness is greatest for these twist angles. These twist angles have the lowest minimum and maximum stiffness values. To see the stiffness of the manipulator at various positions, look at Figure 8. This figure shows that the maximum minimum stiffness criteria for dexterity and workspace performance are not reached, as shown. Depending on the activities to be done, stiffness indices may be used to analyse how effectively the PKM's architectural optimization is performing for machine tool applications.

Stiffness interpretation via eigenscrew decomposition

To find out how stiff the structure is, we'll perform an eigenscrew matrix decomposition. Twists are represented in the axis coordinate system, whereas wrenches are represented in the ray coordinate system. If you want to get relevant answers from the stiffness matrix eigenscrew issue, you must formulate it consistently. Some situations need the use of ray or axis screw-based coordinates. It also assures that the findings are not reliant on the coordinate frame and that the units are maintained as they should be. The findings won't hold up without this step, therefore it's of no real consequence. The bD matrix may be used to transition between two distinct types of coordinate systems.

Table 3
Spring constant and geometrical connection for each screw spring

Spring	$k \times 10^{-8}$	\mathbf{n}^T	\mathbf{r}^T	p
s_1	1.1361	[0, 0, 1]	[0, 0, 0]	-0.0148
s_2	1.1361	[0, 0, 1]	[0, 0, 0]	0.0148
s_3	0.4545	[0.8801, 0.4749, 0]	[0, 0, -0.1118]	-0.0166
s_4	0.4545	[-0.8262, -0.5634, 0]	[0, 0, -0.1118]	0.0166
s_5	0.4545	[-0.0236, -0.9997, 0]	[0, 0, -0.1118]	-0.0166
s_6	0.4545	[-0.0247, -0.9997, 0]	[0, 0, -0.1118]	0.0166

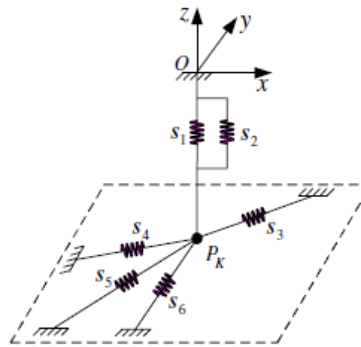


Fig. 9. The physical interpretation of the stiffness of a 3-PUU PKM.

In terms of importance, the number 2 is paramount. Therefore, the spring constant k , the helical joint pitch p , and the geometrical connection parameters n and r determine the spring characteristics of each screw spring. No question, the first two springs are perpendicular to one another and in the same plane as one another, but the final four are perpendicular to one another and on the "z-plane." The centre of stiffness, where rotations and translations may be decoupled to the greatest extent possible, is represented by six springs connected at a single point.

Compliant axis determination

[18] In order to produce a compliant axis, the linear deformation must be parallel to the rotational deformation surrounding it. Only a compliant axis can address the eigenscrew issue. There must be two collinear screws with equal stiffness and opposing signs in order for a compliant shaft to operate. The two collinear eigenscrews define the compliant axis.

Conclusions

The reciprocal screw theory, which accounts for the effects of actuation and restriction on a Jacobian overall, is used in its construction. Additionally, a model of the manipulator's stiffness is built that incorporates both actuators and legs. PKM stiffness may be evaluated using the lowest and greatest eigenvalues of the stiffness matrix in a cubic form useable workspace. This document includes design issues that impact the stiffness of a building's 3-PUU PKM. Deconstructing the stiffness matrix using eigenscrews is the best way to understand the PKM's compliant behaviour. Stiffness may be measured by suspending a body from a series of screw springs in a certain way. Since the PKM's rigidity centre and compliant axis always point in the same direction, it has a larger z-axis stiffness. We have made great progress in our knowledge of 3-PUU PKM stiffness modelling, the assessment of PKM stiffness using architectural characteristics, and a physical interpretation of PKM stiffness. Further parallel manipulators may be simulated using the analytical methodologies described here. The stiffness qualities of the 3-PUU PKM may be used as a starting point for architectural design. An experiment is needed to verify the findings of the stiffness investigation once the PKM is built and produced.

References

[1] J.-P. Merlet, *Parallel Robots*, Kluwer Academic Publishers, London, 2000.

- [2] M. Carricato, V. Parenti-Castelli, A family of 3-DOF translational parallel manipulators, *ASME J. Mech. Des.* 125 (2) (2003) 302–307.
- [3] D. Chablat, P. Wenger, F. Majou, J.-P. Merlet, An interval analysis based study for the design and the comparison of three-degrees-of-freedom parallel kinematic machines, *Int. J. Robot. Res.* 23 (6) (2004) 615–624.
- [4] Y. Li, Q. Xu, Kinematic analysis and design of a new 3-DOF translational parallel manipulator, *ASME J. Mech. Des.* 128 (4) (2006) 729–737.
- [5] L.W. Tsai, S. Joshi, Kinematics analysis of 3-DOF position mechanisms for use in hybrid kinematic machines, *ASME J. Mech. Des.* 124 (2) (2002) 245–253.
- [6] Y. Li, Q. Xu, A new approach to the architecture optimization of a general 3-PUU translational parallel manipulator, *J. Intell. Robot. Syst.* 46 (1) (2006) 59–72.
- [7] S. Huang, J.M. Schimmels, Minimal realizations of spatial stiffnesses with parallel or serial mechanisms having concurrent axes, *J. Robot. Syst.* 18 (3) (2001) 135–146.
- [8] C. Gosselin, Stiffness mapping for parallel manipulators, *IEEE Trans. Robot. Automat.* 6 (3) (1990) 377–382.
- [9] N. Simaan, M. Shoham, Stiffness synthesis of a variable geometry six-degrees-of-freedom double planar parallel robot, *Int. J. Robot. Res.* 22 (9) (2003) 757–775.
- [10] T. Huang, X. Zhao, D.J. Whitehouse, Stiffness estimation of a tripod-based parallel kinematic machine, *IEEE Trans. Robot. Automat.* 18 (1) (2002) 50–58.
- [11] M. Ceccarelli, G. Carbone, A stiffness analysis for CaPaMan (Cassino Parallel Manipulator), *Mech. Mach. Theory* 37 (5) (2002) 427–439.
- [12] S.A. Joshi, L.W. Tsai, Jacobian analysis of limited-DOF parallel manipulators, *ASME J. Mech. Des.* 124 (2) (2002) 254–258.
- [13] S. Bhattacharyya, H. Hatwal, A. Ghosh, On the optimum design of Stewart platform type parallel manipulators, *Robotica* 13 (2) (1995) 133–140.
- [14] B.S. El-Khasawneh, P.M. Ferreira, Computation of stiffness and stiffness bounds for parallel link manipulators, *Int. J. Mach. Tools Manuf.* 39 (2) (1999) 321–342.
- [15] X.-J. Liu, Z.-L. Jin, F. Gao, Optimum design of 3-DOF spherical parallel manipulators with respect to the conditioning and stiffness indices, *Mech. Mach. Theory* 35 (9) (2000) 1257–1267.
- [16] H. Lipkin, J. Duffy, Hybrid twist and wrench control for a robotic manipulator, *ASME J. Mech. Transm. Autom. Des.* 110 (1988) 138–144.
- [17] S. Huang, J.M. Schimmels, The eigenscrew decomposition of spatial stiffness matrix, *IEEE Trans. Robot. Autom.* 16 (2) (2000) 146–156.
- [18] T. Patterson, H. Lipkin, A classification of robot compliance, *ASME J. Mech. Des.* 115 (3) (1993) 581–584.
- [19] Y. Li, Q. Xu, Kinematics and stiffness analysis for a general 3-PRS spatial parallel mechanism, in: *Proceedings of 15th CISMIFTOMMSymposium on Robot Design, Dynamics and Control*, 2004, Rom04-15.
- [20] J.-P. Merlet, Solving the forward kinematics of a Gough-type parallel manipulator with interval analysis, *Int. J. Robot. Res.* 23 (3) (2004) 221–235.